Screening and Simulation Study of Efficacious Antiviral Cannabinoid Compounds as Potential Agents Against SARS-CoV-2

Mahima Devi[a] and Vivek Kumar Yadav[b*]

(a) Department of Bio-informatics, University of Allahabad, Prayagraj, UP 221001, India

(b) Department of Chemistry, University of Allahabad, Prayagraj, UP 221001, India

The proliferation of severe acute respiratory syndrome corona-virus 2 (SARS-CoV-2) and the persistent corona-virus disease 2019 (COVID-19) pandemic emphasize the necessity for novel treatments. Among the diverse pharmacological agents under scrutiny, cannabinoids have garnered attention for their potential antiviral properties. This study utilizes molecular docking and simulation techniques to explore the interaction between cannabinoids drugs and essential SARS-CoV-2 viral proteins, aiming to identify potential therapeutic effects. The results suggest favorable binding energies between certain cannabinoids drugs and viral proteins, especially at the active sites of the spike protein. Our computational findings reveal that the ligands Cannabiscitrin and Cannabisin D exhibit the highest binding affinity (approximately -9.11 and –8.84 kcal/mol, respectively) toward the SARS-CoV-2 receptor, while Alacepril displays the lowest affinity (–6.32 kcal/mol) for the SARS-CoV-2 receptor. The findings suggest a potential inhibitory effect of cannabinoid drugs on both viral entry and replication. Furthermore, simulations demonstrate cannabinoid binding to the CB2 receptor, suggesting potential immunomodulatory roles in SARS-CoV-2 infection. This research underscores the promise of cannabinoids as SARS-CoV-2 therapeutic agents, necessitating further validation and clinical exploration.

1 Introduction

The world stood witness to an unprecedented and deadly outbreak of COVID-19, a disease caused by the severe acute respiratory syndrome corona-virus 2 (SARS-CoV-2) [1]. Originating in Wuhan City, Hubei, China, this virulent virus quickly traversed borders and infected populations worldwide [2,3]. COVID-19 is characterized by a spectrum of symptoms, ranging from respiratory distress, fever, and pneumonia to sore throats and lung infections [4,5]. Recognizing the gravity of the situation, WHO declared the COVID-19 outbreak a Public Health Emergency of International Concern on January 30th, 2020 [6]. As of June 22, 2020, the WHO had documented a staggering 8,860,331 confirmed cases and 465,740 deaths worldwide, underscoring the magnitude of the pandemic [7]. Globally, as of 8 November 2023, there have been 772,166,517 (about 45,001,575 in India) confirmed cases of COVID-19, including 6,981,263 (about 533,295 in India) deaths, reported to WHO [8]. Even with the recent availability of vaccines, SARS-CoV-2 continues to spread rapidly [9], emphasizing the necessity for alternative treatments, particularly for populations with limited inclination or access to vaccines. To date, only a limited number of therapies have been identified that can effectively block SARS-CoV-2 replication and viral production [10].

The search for effective antiviral agents against SARS-CoV-2 has become an urgent priority, necessitating the exploration of diverse pharmacological compounds [11]. Cannabinoids, a class of compounds primarily derived from the Cannabis sativa plant, have garnered substantial attention due to their broad pharmacological effects, including anti-inflammatory, immunomodulatory, and potential antiviral properties [12,13]. In cannabinoids, the Cannabinoid type 2 (CB2) ligands, a class of compounds that interact with the CB2 receptors in the endocannabinoid system, have shown promising antiviral activity [14–16]. These ligands exhibit a potential inhibitory impact on viral entry and replication, suggesting a role in impeding the spread of viruses [17–20]. Particularly relevant to the ongoing challenges posed by SARS-CoV-2, simulations have revealed the binding of cannabinoids to the CB2 receptor, indicating their potential immunomodulatory roles in combating viral infections [21–24]. The exploration of CB2 ligands as antiviral agents represents a novel avenue in the quest for effective treatments against viral pathogens [25]. Recent research has suggested that cannabinoids may hold promise as agents capable of mitigating viral infections [26,27]. Despite multiple studies and various unverified claims regarding CBD-containing products, the biological actions of CBD itself remain unclear, and specific targets are largely unknown [28]. While limited, certain studies have reported that particular cannabinoids demonstrate antiviral effects against viruses such as the hepatitis C virus and others [29]. The cannabis plant contains over 550 chemical constituents, with approximately 150 being cannabinoids and more than 400 non-cannabinoids [30]. The primary pharmacologically active compounds include the psychoactive tetrahydrocannabinols (THC), such as Δ^8-THC and Δ^9-THC, along with non-psychoactive cannabinoids like cannabinol (CBN), cannabidiol (CBD), and cannabigerol (CBG), among others [31–34].

This paper presents a comprehensive investigation into the potential of certain cannabinoid compounds as antiviral agents against SARS-CoV-2 through a combination of screening and simulation techniques. The favorable binding interactions observed between selected cannabinoids and viral proteins suggest their ability to interfere with critical viral processes. Moreover, the binding of cannabinoids to the CB2 receptor highlights their potential immunomodulatory properties, which may play a crucial role in reg-

*Corresponding author Email: vkyadav@alldunivac.in

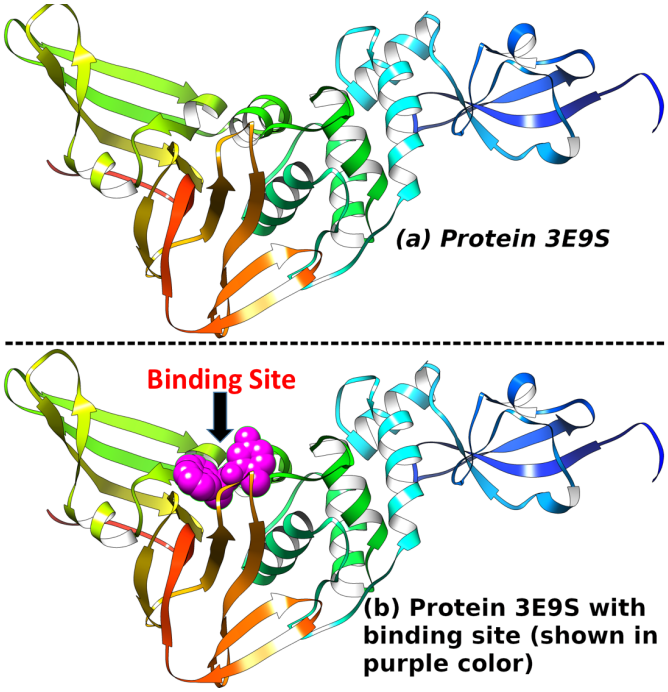

Fig. 1 SARS-CoV-2 protein structure (PDB ID: 3E9S) (a) without and (b) with binding site, respectively.

ulating the immune response during SARS-CoV-2 infection. Further experimental studies are warranted to validate these findings and explore the clinical implications of cannabinoid-based therapies in combating COVID-19. Finally, we conclude with a succinct summary of our significant findings obtained throughout this study.

2 Methodology

2.1 Preparation of Protein and selection of ligands

The 3D crystal structure of the SARS-CoV-2 receptor binding domain (RBD) of the spike protein complexed with the human ACE2 receptor (PDB ID: 3E9S) and Cannabinoid type-2 receptor (PDB ID: 2YDO), were downloaded from th0e RCSB Protein Data Bank (PDB) [35]. To get pure protein, all ligands attached are removed using PyMOL software and saved the processed file in PDB format [36]. To avoid the interference of water molecules in the pocket region, we used auto-dock tools [37] that deleted water molecules from 3D structure of nucleoprotein. Then polar hydrogen atoms are added in the protein. Further, the protein structure was prepared for drug docking using AutoDockTools software [37]. Hydrogen atoms were added to the protein, and non-polar hydrogens were merged. The polar hydrogen charges were then assigned using the Gasteiger method. The protein was then saved in the PDBQT format, which is compatible with the AutoDockVina software used for molecular docking simulations. The cannabinoid ligands selected for this study were Cannabis. These compounds were chosen because they have been previously reported to have antiviral properties and are easily accessible for experimental studies [15,16]. The 3D structure of the eight compounds was downloaded in SDF format via the ZINC database [38] and details are reported in Table 1. Choose ligand and then select molecule for auto-dock. Next step is to save as pdbqt file. Now we have the files Cannabinol.pdbqt and Cannabiscitrin.pdbqt. In this way, second step of docking is completed. Fig. 2 shows the prepared view of ligand Alacepril, Myricetin, Cannabidiol Acid, Cannabigerol,Cannabigerolic Acid, and Cannabisin D are also prepared using the same procedure.

2.2 Molecular docking methodology

Molecular docking were performed using the Auto-Dock Vina software [39]. The protein structure of the SARS-CoV-2 RBD and Cannabinoid type-2 receptor were used as the target proteins, while the cannabinoid drugs were used as the ligands. For 3E9S, the grid box was defined to encompass the entire RBD protein with a size of 60 x 60 x 60 $Å^3$, a grid spacing of 0.5 Å, and x, y, z center grid box (-31.02, 21.89, 30.09). For 2YDO the grid box was defined to encompass the entire RBD protein with a size of 60 x 60 x 60 $Å^3$, a grid spacing of 0.572 $Å^3$ and x, y, z center grid box (-35.02, 6.109, -21.757). The exhaustiveness parameter was set to 50, which is the maximum number of binding modes to be searched. The binding energies of the docked complexes were calculated and ranked according to their binding affinity, expressed in kcal/mol. The lowest binding energy (more negative energy) conformation was considered the most energetically favorable and was selected for further analysis. The interactions between the cannabinoids and the amino acid residues of the SARS-CoV-2 RBD and cannabinoid type-2 were analyzed, and the binding modes were compared to identify the most favorable binding mode. The binding affinity of each ligand was calculated and compared.

2.3 Molecular dynamics simulation methodology

After the molecular docking, the SARS-CoV-2 RBD and cannabinoid type-2 complexed with the best docked ligands was subjected to molecular dynamics (MD) simulation using the GROMACS software [40]. The system was first energy minimized using the steepest descent algorithm with a maximum of 5000 steps or until a convergence threshold of 1000 kJ/mol was reached. The MD simulation was carried out using the CHARMM36 force field [41]with the Particle Mesh Ewald (PME) method for long-range electrostatic interactions. The time step was set to 2 fs, and the temperature and pressure were maintained at 300 K and 1 bar, respectively, using the Nose-Hoover thermostat and the Parrinello-Rahman barostat [42–44]. The system was simulated for 50 ns, and the trajectories were saved every 10 ps for analysis. The stability and convergence of the MD simulations were assessed by monitoring the root mean square deviation (RMSD) of the protein-ligand complex and the root mean square fluctuation (RMSF) of the protein backbone residues. The equations are as

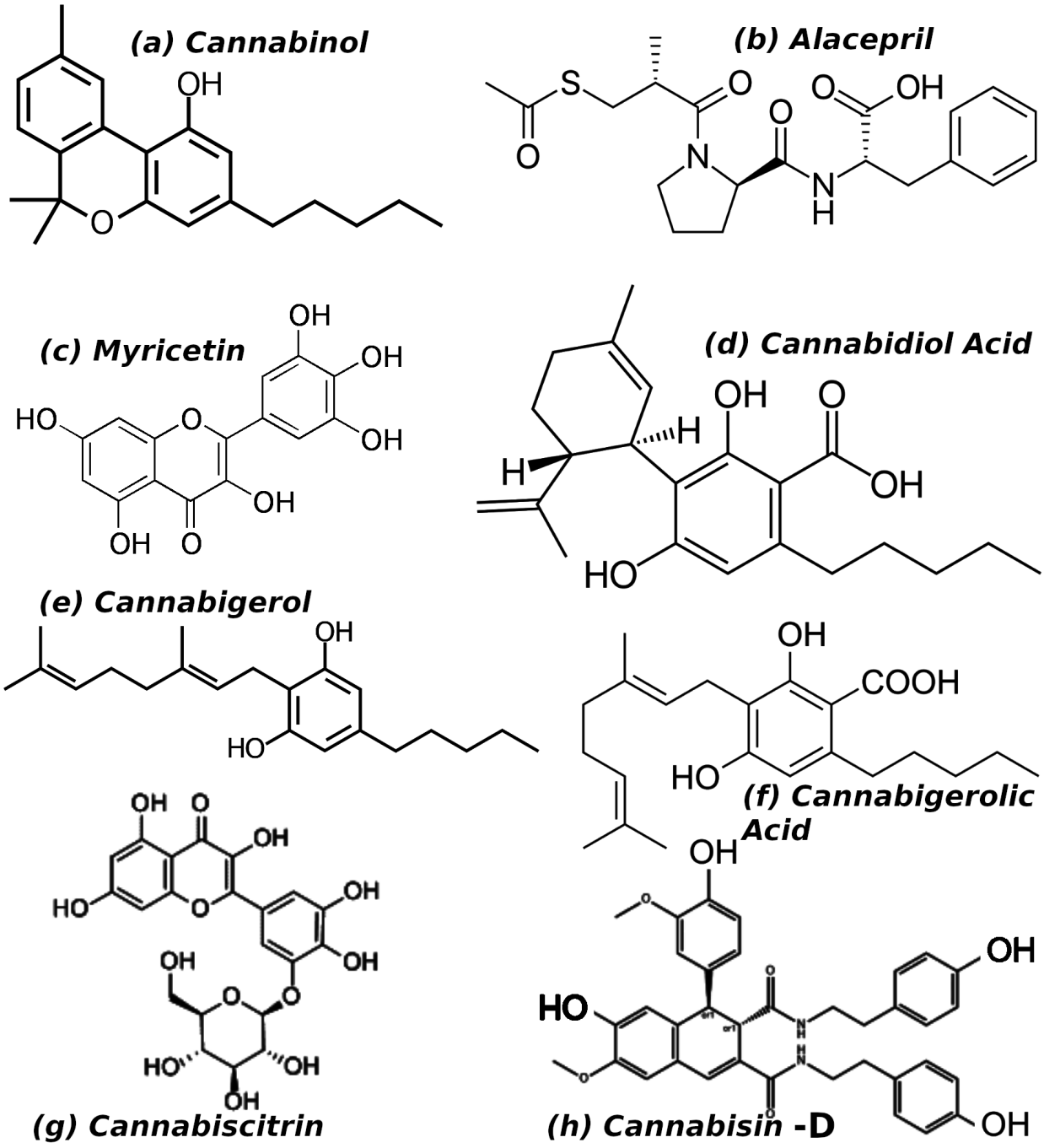

Fig. 2 2D structure of the eight Cannabinoid ligands

S.No.	Compound	ZINC ID	Molecular formula	Mole. Wt.	HBD	HBA	Antiviral activity (Study)
1	Cannabinol	1530833	C21H26O2	310.437	1	2	Yes (In vitro)
2	Alacepril	3775143	C20H26N2O5S	406.504	1	6	Yes (In vitro)
3	Myricetin	3874317	C15H10O8	318.237	4	8	Yes (In vitro)
4	Cannabidiol Acid	4098864	C22H30O4	358.478	2	4	Yes (In vitro)
5	Cannabigerol	4217650	C21H32O2	316.485	2	2	Yes (In vitro)
6	Cannabigerolic Acid	8773249	C22H32O4	360.494	2	4	Yes (In vitro)
7	Cannabiscitrin	14436714	C21H20O13	480.378			Yes (In vitro)
8	Cannabisin D	44307185	C36H36NO8	624.69	6	8	Yes (In vitro)

Table 1 The molecular formula, molecular weight, hydrogen bond donor, hydrogen bond acceptor, rotatable bonds, and ZINC ID of eight compounds.

follows:

$$RMSD_X = \sqrt{\frac{1}{N}\sum_{i=1}^{N}\left(r_i(t_x) - r_i(t_{ref})\right)^2}$$
$$RMSF_i = \sqrt{\frac{1}{T}\sum_{t=1}^{T}\left(r_i(t) - r_i(t_{ref})\right)^2} \quad (1)$$

where In RMSD equation, N is the number of chosen atoms, t_{ref} is correspond to reference time and generally set to 0 for first frame, r_i is the position of the selected atoms belong to the frame x recorded at time t_x. To calculated RMSD this procedure is repeated for every frame along the simulation trajectory. In RMSF equation, t is termed as trajectory time over which RMSF is calculated, reference time is denoted by t_{ref}, r_i is position of residue I, and angular bracket denotes the average over the selection of atoms in the residue. The MD trajectories were analyzed using GROMACS tools and visualized using PyMOL[36] and VMD[45]. The ligand-protein interactions and the conformational changes of the protein-ligand complex over the simulation time were analyzed and compared between the different cannabinoid compounds.

3 Results and discussion

3.1 Docking Analysis

The molecular docking of all eight cannabinoid drugs with the 3E9S and 2YDO receptors has been performed. Several cannabinoid compounds exhibited favorable binding affinities to the SARS-CoV-2 RBD, suggesting their potential as inhibitors of the virus. The binding energies of the top-performing cannabinoid compounds, such as Cannabiscitrin and Cannabisin D, are -9.11 to -8.84 kcal/mol, respectively, indicating strong and favorable binding affinity. These two compounds also demonstrate a stronger binding affinity with the cannabinoid type 2 receptor, with binding energies of -10.26 and -11.22 kcal/mol. Our results for all ligands with 3E9S and 2YDO proteins show a similar binding trend. If a ligand displays a weaker interaction with 2YDO, it also exhibits a weaker interaction with 3E9S, and vice versa. The binding modes analysis revealed that both Cannabiscitrin and Cannabisin D compounds interact efficiently with the 3E9S and 2YDO with multiple interacting site with in the binding pocket. In Figure 4(a,b), the ligand Cannabiscitrin shows hydrophobic interaction with the residues 62PRO, 68ARG, 71ALA, and 82PHE inside the binding pocket of 3E9S. Whereas the residues 77THR and 83LEU displays the H-bonding with the ligand. The residue π-Cation Interactions was found between 68ARG and the Cannabiscitrin ligand. For the case of Cannabisin D as shown in Figure 4(c,d), the residues 249PRO, 250PRO, 266TYR, 270TYR, 271GLN, and 275TYR grabs the ligand by hydrophobic interaction. The ligand also gets stabilized inside the binding pocket with direct hydrogen bonding with 164LEU, 169GLU, and 270TYR. This Cannabisin D ligand also shows π-Cation Interactions with the 168ARG residue of 3E9S protein. Similar binding mode analysis has been performed to elucidate the behavior of Cannabiscitrin and Cannabisin D inside the binding site of the cannabinoid type 2 receptor (See Figure SI2). It was found that the Cannabiscitrin shows hydrophobic interactions mainly with 168PHE, 246TRP, 249LEU, and 274ILE residues of the target protein. The ligand also shows H-bond interaction with 66ILE, 169GLU, and 253ASN whereas the 168PHE displays the $\pi - \pi$ interaction with the Cannabiscitrin ligand. Similarly, for the case of Cannabisin D inside the binding pocket, the residues 66ILE, 84VAL, 167LEU, 168PHE, 169GLU, 249LEU, 267LEU,and 274ILE shows hydrophobic interaction with docked ligand. The ligand also makes six H-bond with 150LYS, 153LYS, 168PHE, 169GLU, 253ASN, and 278HIS residues of the receptors which plays a vital role in stabilizing the ligand inside the binding pocket of 2YDO. Apart form this, the ligand also shows $\pi - \pi$ interaction with the 168PHE residue of target protein (See Figure SI2). We performed the similar analysis for all the ligand used in the present study and the details of the interaction with both the proteins are presented in SI (See Ligand Interaction Diagrams and Table for residue details). Overall, these results suggest that Cannabiscitrin and Cannabisin D have the potential to be inhibitors of the SARS-CoV-2 virus by binding to the RBD of the virus, and further studies are needed to validate these findings and evaluate their efficacy as COVID-19 therapeutics.

3.2 Dynamical Analysis

MD simulations are performed on best-docked Cannabiscitrin ligand with receptors "3E9S," and "2YDO," and the temperature, pressure, and energy are monitored throughout the 50ns of

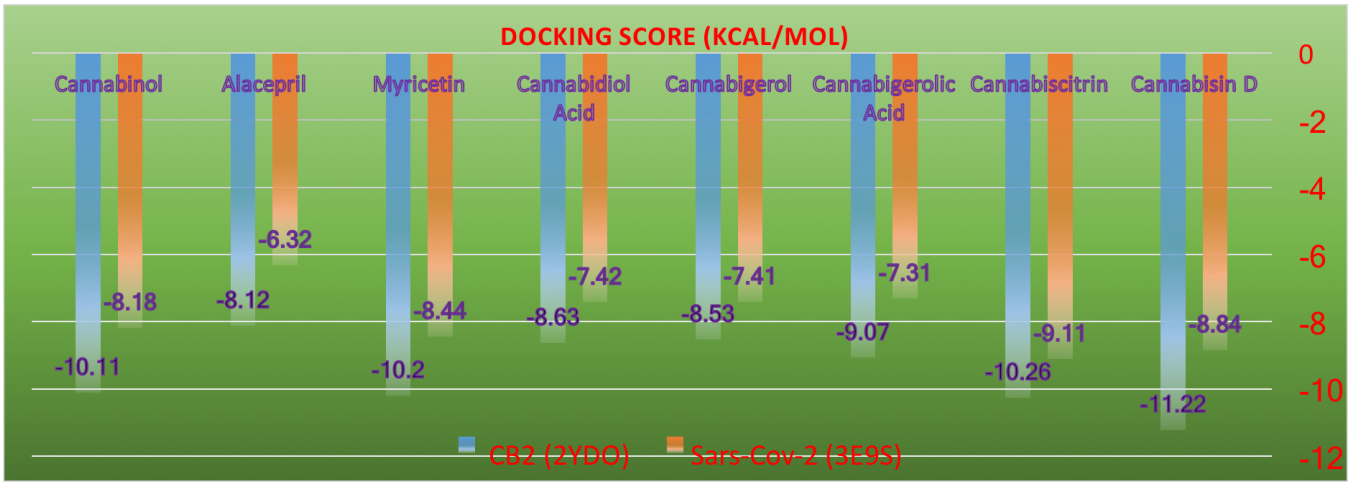

Fig. 3 Docking score for all eight ligands with both proteins

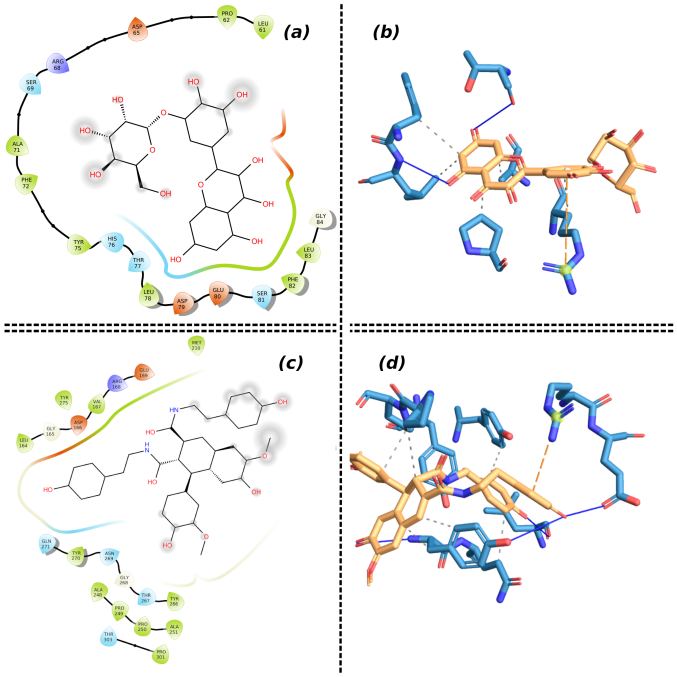

Fig. 4 (a),(c) are 2D Ligand interaction diagram and (b),(d) are 3D Protein ligand interaction of Cannabiscitrin and Cannabisin D with 3E9S, respectively.

simulation trajectory (Figure SI 5). It is essential that these quantities should remain constant throughout the simulations which is the key requirement for the stability of the simulations. It is clearly shown in Figure SI 5 that the simulation is stable and not deviating from the initial structure as all the above-mentioned quantities are fluctuating around the mean initial value. The energy plotted in this figure is the sum of the both kinetic and potential energy of the system. The energy is plotted in arbitrary units (a.u.), the temperature in Kelvin (K), and pressure in atm. The results for 3E9S and 2YDO are shown for 50 ns which is stable and good enough to compute the various dynamical properties. We can conclude from the Figure that, when the temperature is on the higher side then the energy of the system also shoots towards the larger values and vice-versa.

RMSD (Root Mean Square Deviation) analysis is a widely used method to measure the structural similarity between two protein structures. It quantifies the average displacement between corresponding atoms in two protein conformations or between a reference structure and a set of structures. The RMSD for ligand inside the protein 2YDO as represented by black line demonstrates that after some initial conformational change (adjustment of ligand in the presence of water) becomes stable and remains at the same comfort zone throughout the simulations. For the cases of 3E9S protein-ligand systems, there is also small fluctuation in RMSD as the ligands in the 3E9S is more exposed to surrounding water compared to 2YDO where the ligands are sitting well inside the binding pocket of protein as shown in figure 5a. We conclude from this RMSD result that all the ligands get stable after some initial conformation change and remain near the binding site throughout the course of simulations as predicted from the molecular docking.

An area of the structure with high RMSF (Figure 5b) values frequently diverges from the average, indicating high mobility. When RMSF analysis is carried out on proteins, it is typically restricted to backbone or alpha-carbon atoms; these are more characteristic of conformational changes than the more flexible side chains. The RMSF for the Cα atoms during MD simulation for all the proteins 3E9S, and 2YDO are shown in Figure 5 along

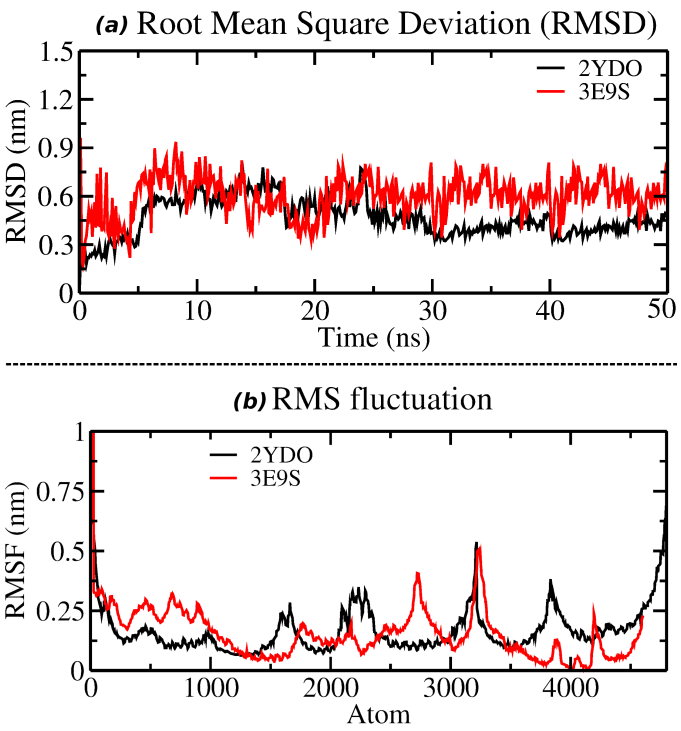

Fig. 5 (a) RMSD values of Ca atoms of native structures of both the proteins. y-axis is RMSD (nm), and the x-axis is time (ns) (b) RMSF values of the carbon alpha over the entire simulation. y-axis is RMSF (nm), and the x-axis is residue.

with RMSD plot.

A hydrogen bond is formed by the interaction of a hydrogen atom that is covalently bonded to an electro-negative atom (donor) with another electro-negative atom (acceptor). Hydrogen bonding confers rigidity to the protein structure and specificity to intermolecular interactions. Hydrogen bonds are crucial in molecular interactions, particularly in biological systems, as they play a significant role in stabilizing protein structures. We analyze the hydrogen bonds (H-bonds) between all possible donors (D) and acceptors (A) using the gmxhbond program of GROMACS. To determine, if an H-bond exists, a geometrical criterion of r =< rHB = 0.35 nm and an angle cut off of 30° is used. The receptors 3E9S, and 2YDO exhibit a consistent range of hydrogen bonds between 0 to 3 throughout the entire simulation. It is clear from the simulation that the ligand-protein docked structure shows stability during the course of simulation by retaining the similar number of hydrogen bonds with minor fluctuation.

Solvent-accessible surface area (SASA) is another crucial property that provides information about the overall protein conformation in an aqueous environment. Proteins consist of hydrophobic and hydrophilic residues and tend to adopt structures that minimize the exposure of hydrophobic residues to the aqueous solvent. Increases in SASA from a stable state can indicate protein instability, such as unfolding that exposes hydrophobic residues to the solvent, leading to undesirable changes like irreversible aggregation. The substitution of amino acids, whether through

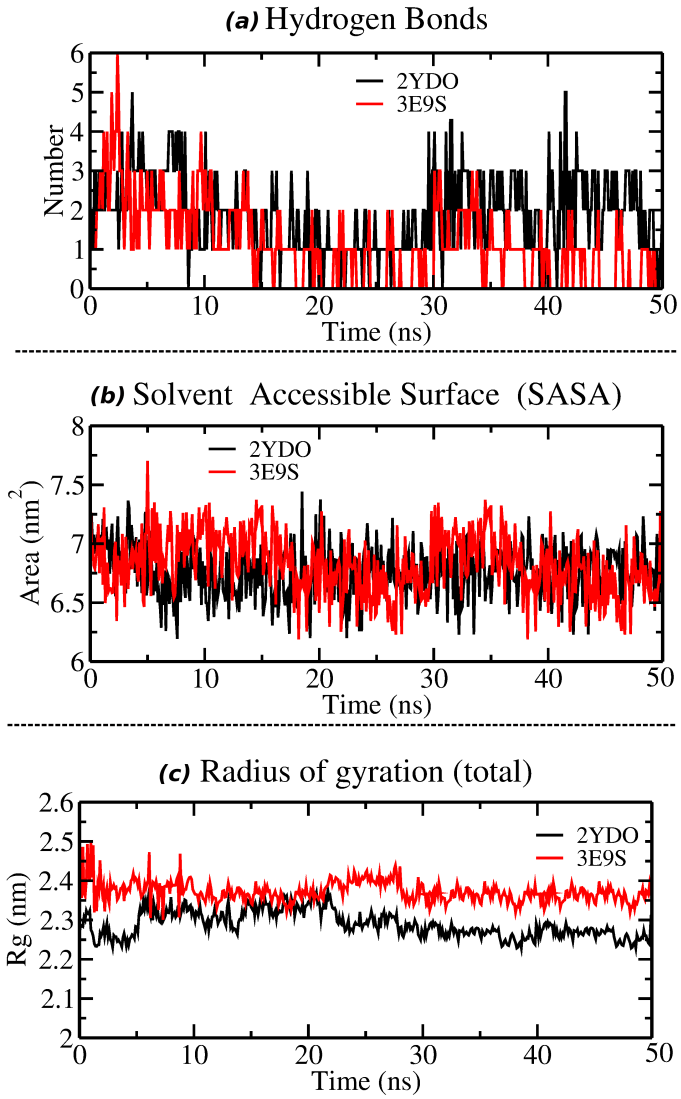

Fig. 6 (a) Total number of H-bond count throughout the simulation, (b) Solvent accessibility of native proteins. y-axis is SASA (nm2), and the x-axis is time (ns), and (c) Rg of both the protein backbone over the entire simulation. y-axis is Rg (nm), and the x-axis is time (ps).

mutational or chemical means, can also disrupt the native conformation of a protein, resulting in partial unfolding and leading to increases in SASA. The SASA value between for our work are ranges between 6.5-10.5 nm^2 as shown in Figure 6 explains that the binding of ligands does not affect the folding of the proteins.

Radius of gyration was determined to determine the system's compactness over time. Higher Rg values indicate less compactness (more unfolded) and conformational entropy, whereas low Rg values indicate excellent compactness and structure stability (more folded). The radius of the gyration plot for both docked proteins after running molecular dynamics simulation were shown in Figure 6. The proteins 3E9S, and 2YDO in the complex were stable, with fewer fluctuations in the Rg value ranging from 2.2-2.5 nm, indicating less variation. The radius of gyration results revealed that the binding of these molecules

does not induce structural changes. The plots also show the least fluctuation for 2YDO compared to 3E9S. Overall, these results suggest that Cannabiscitrin can form stable complexes with the SARS-CoV-2 RBD and induce conformational changes that lead to a reduction in the distance between key amino acid residues involved in the binding site.

4 Conclusions

The objective of this study was to identify antiviral cannabinoid type 2 drugs capable of targeting the main protease (Mpro) of SARS-CoV-2. We utilized standard molecular modeling techniques, including molecular docking and molecular dynamics studies. Cannabis sativa is considered one of the most controversial plants in our society; however, at the same time, it has been used worldwide for medicinal purposes for centuries. In this study, we explored the effects of antiviral cannabinoid type-2 drugs on the recent SARS-COV-2 pandemic. We found that Cannabiscitrin is the best-suited lead drug candidate against the nucleoprotein (PDB ID: 3E9S) of Covid-19. This protein is a viral protein. Furthermore, through a comparative study, we found that this drug is the most suitable candidate among other existing lead candidates such as Cannabisin D, Cannabinol, Myricetin, etc. We identified the best molecular docking parameter with a binding affinity value of -9.11, which is higher than that of other leading candidates. The therapeutic potential of Cannabiscitrin as an antiviral agent has been more critical in combating COVID-19, caused by the severe acute respiratory syndrome coronavirus-2. Based on a computational study, we concluded that the Cannabiscitrin drug can better combat the SARS-COV-2 nucleoprotein.

5 Data availability

The data required to reproduce these findings are available from the corresponding author upon reasonable request.

6 Author Contributions

MD and VKY performed calculations, analyzed the results and wrote the manuscript.

7 Acknowledgment

VKY sincerely thanks Prof. Michael L. Klein of Temple University, Philadelphia, USA, for his valuable discussions in setting up the research problem. V.K.Y. acknowledge National Supercomputing Mission (NSM) for providing computing resources of 'PARAM Shivay' at Indian Institute of Technology (BHU), Varanasi, which are implemented by C-DAC and supported by the Ministry of Electronics and Information Technology (MeitY) and Department of Science and Technology (DST), Government of India.

8 Keywords

Docking, antiviral cannabinoid drugs; Sars-CoV-2; Molecular Dynamics.

9 Supplementary Information

See the supplementary material for details on the Cannabinoid Type-2 receptor, ligand interaction diagrams, and a table containing both the residues of the protein and their ligands.

References

1 World Health Organization. WHO Coronavirus disease (COVID-19) dashboard. Retrieved June 22, 2020, from https://covid19.who.int/.

2 Chen, Y. W., Yiu, C. B.,and Wong, K. Y., Prediction of the SARS-CoV-2 (2019-nCoV) 3C-like protease (3CL pro) structure: Virtual screening reveals velpatasvir, ledipasvir, and other drug repurposing candidates. F1000Research, 2020, 9, 129. https://doi.org/10.12688/f1000research.22457.2

3 Chen, Y., Liu, Q., and Guo, D., Emerging coronaviruses: Genome structure, replication, and pathogenesis. Journal of Medical Virology, 2020, **92(4)**, 418–423.

4 Adhikari, S. P., Meng, S., Wu, Y. J., Mao, Y. P., Ye, R. X., Wang, Q. Z., Sun, C., Sylvia, S., Rozelle, S., Raat, H., and Zhou, H., Epidemiology, causes, clinical manifestation and diagnosis, prevention and control of coronavirus disease (COVID-19) during the early outbreak period: A scoping review. Infectious Diseases of Poverty, 2020, **9(1)**, 29.

5 S. R. Weiss, J. L. Leibowitz, Coronavirus pathogenesis. Adv. Virus Res. 2021, **81**, 85–164.

6 Sohrabi, C., Alsafi, Z., O'Neill, N., Khan, M., Kerwan, A., Al-Jabir, A., Iosifidis, C., and Agha, R., World Health Organization declares global emergency: A review of the 2019 novel coronavirus (COVID-19). International Journal of Surgery (London, England), 2020, **76**, 71–76.

7 Chen, Y. W., Yiu, C. B.,and Wong, K. Y., World Health Organization. (2020a). Naming the coronavirus disease (COVID-19) and the virus, 2020,

8 World Health Organization. (2023). https://covid19.who.int/

9 S. E. Galloway, P. Paul, D. R. MacCannell, M. A. Johansson, J. T. Brooks, A. M. Neil, R. B. Slayton, S. Tong, B. J. Silk, G. L. Armstrong, M. Biggerstaff, V. G. Dugan, Emergence of SARS-CoV-2 B.1.1.7 lineage - United States, December 29, 2020-January 12, 2021. MMWR Morb. Mortal. Wkly Rep. 2021, **70**, 95–99.

10 Zhu N, Zhang D, Wang W, et al. A novel coronavirus from patients with pneumonia in China, 2019. New England Journal of Medicine, 2020, **382(8)**, 727-733.

11 Geo, Y. R., Cao, Q. D., Hong, Z. S., Tan, Y. Y., Chen, S. D., Jin, H. J., Tan, K. S., Wang, D. Y., and Yan, Y. The origin, transmission and clinical therapies on coronavirus disease 2019 (COVID-19) outbreak - an update on the status. Military Medical Research, 2020, **7(1)**, 11. https://doi.org/10.1186/s40779-020-00240-0

12 Di Marzo, V., and Piscitelli, F., The endocannabinoid system and its modulation by phytocannabinoids. Neurotherapeutics, 2015, **12(4)**, 692-698.

13 Klein, T. W., Cannabinoid-based drugs as anti-inflammatory therapeutics. Nature Reviews Immunology, 2005, **5(5)**, 400-

411.
14 Edery, H., Grunfeld, Y., Ben-Zvi, Z. and Mechoulam, R., Structural requirements for cannabinoid activity. Ann. N.Y. Acad. Sci., 1971, **191**, 40–53.
15 Gaoni, Y. and Mechoulam, R., Isolation, structure and partial synthesis of an active constituent of hashish. J. Am. Chem. Soc., 1964, **86**, 1646–1647
16 Yadav, V.K., Computational insights into the agonist activity of Cannabinoid receptor type-2 ligands using molecular dynamics simulation. Current Science, 2022, **122**, 167–177.
17 Breemen, R.B.V et. al. Cannabinoids Block Cellular Entry of SARS-CoV-2 and the Emerging Variants. J. Nat. Prod. 2022, **85**, 176-184.
18 Martin, B. R., Balster, R. L., Razdan, R. K., Harris, L. S. and Dewey, W. L., Behavioral comparisons of the stereoisomers of tetra-hydrocannabinols. Life Sci., 1981, **29**, 565–574.
19 Lambert, D. M. and Fowler, C. J., The endocannabinoid system: drug targets, lead compounds and potential therapeutic applications. J. Med. Chem., 2005, **48(16)**, 5059–5087.
20 Pertwee, R. G., The diverse CB1 and CB2 receptor pharmacology of three plant cannabinoids: delta9-tetrahydrocannabinol, cannabidiol and delta9-tetrahydrocannabivarin. British Journal of Pharmacology, 2008, **153(2)**, 199-215.
21 Chen, C.; Liang, H.; Deng, Y.; Yang, X.; Li, X.; Hou, C. Analysis and Identification of Bioactive Compounds of Cannabinoids in Silico for Inhibition of SARS-CoV-2 and SARS-CoV. Biomolecules 2022, **12**, 1729.
22 Pereira CF, Vargas D, Toneloto FL, Ito VD, Volpato RJ. Implications of Cannabis and Cannabinoid Use in COVID-19: Scoping Review. Rev Bras Enferm. 2022;75(Suppl 1):e20201374. https://doi.org/10.1590/0034-7167-2020-1374
23 Paland N, Pechkovsky A, Aswad M, Hamza H, Popov T, Shahar E and Louria-Hayon I., The Immunopathology of COVID-19 and the Cannabis Paradigm. Front. Immunol. 2021, **12**, 631233. doi: 10.3389/fimmu.2021.631233
24 Perez, R.; Glaser, T.; Villegas, C.; Burgos, V.; Ulrich, H.; Paz, C. Therapeutic Effects of Cannabinoids and Their Applications in COVID-19 Treatment. Life 2022, **12**, 2117. https://doi.org/10.3390/life12122117
25 Nguyen L.C., Yang D., Nicolaescu V., et. al., Cannabidiol inhibits SARS-CoV-2 replication through induction of the host ER stress and innate immune responses. Sci Adv., 2022, **8**, eabi6110, doi: 10.1126/sciadv.abi6110.
26 Olah, A., Markovics, A., Szabó-Papp, J., et al., Differential effectiveness of selected non-psychotropic phytocannabinoids on human sebocyte functions implicates their introduction in dry/seborrhoeic skin and acne treatment. Experimental Dermatology, 2016, **25(9)**, 701-707.
27 Raj, V. S., Mou, H., Smits, S. L., et al., Dipeptidyl peptidase 4 is a functional receptor for the emerging human coronavirus-EMC. Nature, 2013, **495**, 251-254.
28 K. M. Nelson, J. Bisson, G. Singh, J. G. Graham, S. N. Chen, J. B. Friesen, J. L. Dahlin, M. Niemitz, M. A. Walters, G. F. Pauli, The essential medicinal chemistry of cannabidiol (CBD). J. Med. Chem. 2020, **63**, 12137–12155.
29 H. I. Lowe, N. J. Toyang, W. McLaughlin, Potential of cannabidiol for the treatment of viral hepatitis. Pharm. Res., 2017, **9**, 116–118.
30 Mahmud, M.S.; Hossain, M.S.; Ahmed, A.T.M.F.; Islam, M.Z.; Sarker, M.E.; Islam, M.R. Antimicrobial and Antiviral (SARS-CoV-2) Potential of Cannabinoids and Cannabis sativa: A Comprehensive Review. Molecules 2021, **26**, 7216. https://doi.org/ 0.3390/molecules26237216
31 RECOVERY. No Clinical Benefit From Use of Lopinavir-Ritonavir in Hospitalised COVID-19 Patients Studied in RECOVERY. (2020). Available online at: https://www.recoverytrial.net/news/no-clinical-benefit-from- use-of-lopinavir-ritonavir-in-hospitalised-covid-19-patients-studied-in-recovery (accessed September 14, 2020).
32 Group RC, Horby P, Mafham M, Linsell L, Bell JL, Staplin N, et al. Effect of hydroxychloroquine in hospitalized patients with Covid-19. N Engl J Med. (2020) **383:203**, 1–40. doi: 10.1056/NEJMoa2022926
33 Agarwal A, Mukherjee A, Kumar G, Chatterjee P, Bhatnagar T, Malhotra P. Convalescent plasma in the management of moderate covid-19 in adults in India: open label phase II multicentre randomised controlled trial (PLACID Trial). Br Med J., 2020, **371**, 3939. doi: 10.1136/bmj.m3939
34 Paland, N., Pechkovsky, A., Aswad, M., Hamza, H., Popov, T., and Shahar, E. (2021). The Immunopathology of COVID-19 and the Cannabis Paradigm. Front Immunol. 2021, **12**, 631233.
35 https://www.rcsb.org/.
36 https://pymol.org/2.
37 Morris G.M., Huey R., Lindstrom W., Sanner M.F., Belew R.K., Goodsell D.S., Olson A.J. AutoDock4 and AutoDockTools4: automated docking with selective receptor flexibility. J. Comput. Chem. 2009, **30**, 2785–2791.
38 John J. Irwin and Brian K. Shoichet, ZINC – A Free Database of Commercially Available Compounds for Virtual Screening. J Chem Inf Model, 2005, **45**, 177–182.
39 Trott O., Olson A.J. AutoDock Vina: improving the speed and accuracy of docking with a new scoring function, efficient optimization, and multithreading. J. Comput. Chem. 2010, **31**, 455–461. doi: 10.1002/jcc.21334.
40 Van Der Spoel D., Lindahl E., Hess B., Groenhof G., Mark A.E., Berendsen H.J.C. GROMACS: fast, flexible, and free. J. Comput. Chem. 2005;26:1701–1718. doi: 10.1002/jcc.20291.
41 Par Bjelkmar, Per Larsson, Michel A. Cuende, Berk Hess, and Erik Lindahl, Implementation of the CHARMM Force Field in GROMACS: Analysis of Protein Stability Effects from Correction Maps, Virtual Interaction Sites, and Water. Chem. Theory Comput., 2010, **6(2)**, 459–466.
42 S. Nose, A molecular dynamics method for simulations in the canonical ensemble, Mol. Phys., 1984, **52**, 255–268.
43 W.G. Hoover, Canonical dynamics: Equilibrium phase-space distributions, Phys. Rev. A, 1985, **31**, 1695–1697.

44 M. Parrinello and A. Rahman, “Polymorphic transitions in single crystals: A new molecular dynamics method,” J. Appl. Phys., 1981, **52**, 7182–7190.

45 Humphrey, W., Dalke, A. and Schulten, K., VMD - Visual Molecular Dynamics, J. Molec. Graphics, 1996, **14**, 33-38.

Supporting Information

Screening and Simulation Study of Efficacious Antiviral Cannabinoid Compounds as Potential Agents Against SARS-CoV-2

Mahima Devi[a] and Vivek Kumar Yadav[*,b]

(a) Department of Bio-informatics, University of Allahabad, Prayagraj, UP 221001, India
(b) Department of Chemistry, University of Allahabad, Prayagraj, UP 221001, India

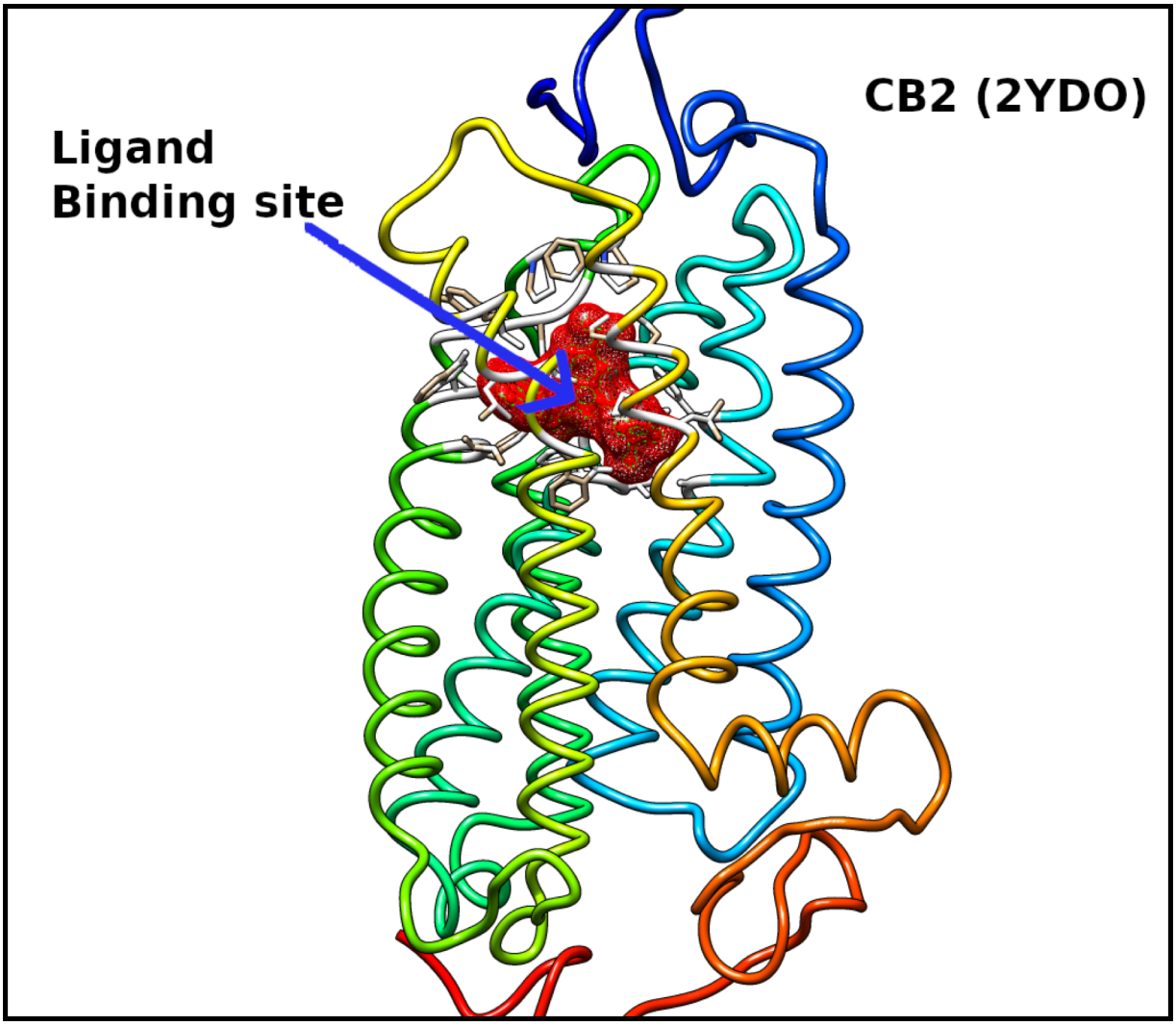

Figure SI-1: Structure of CB2 receptor with highlighted ligand binding site.

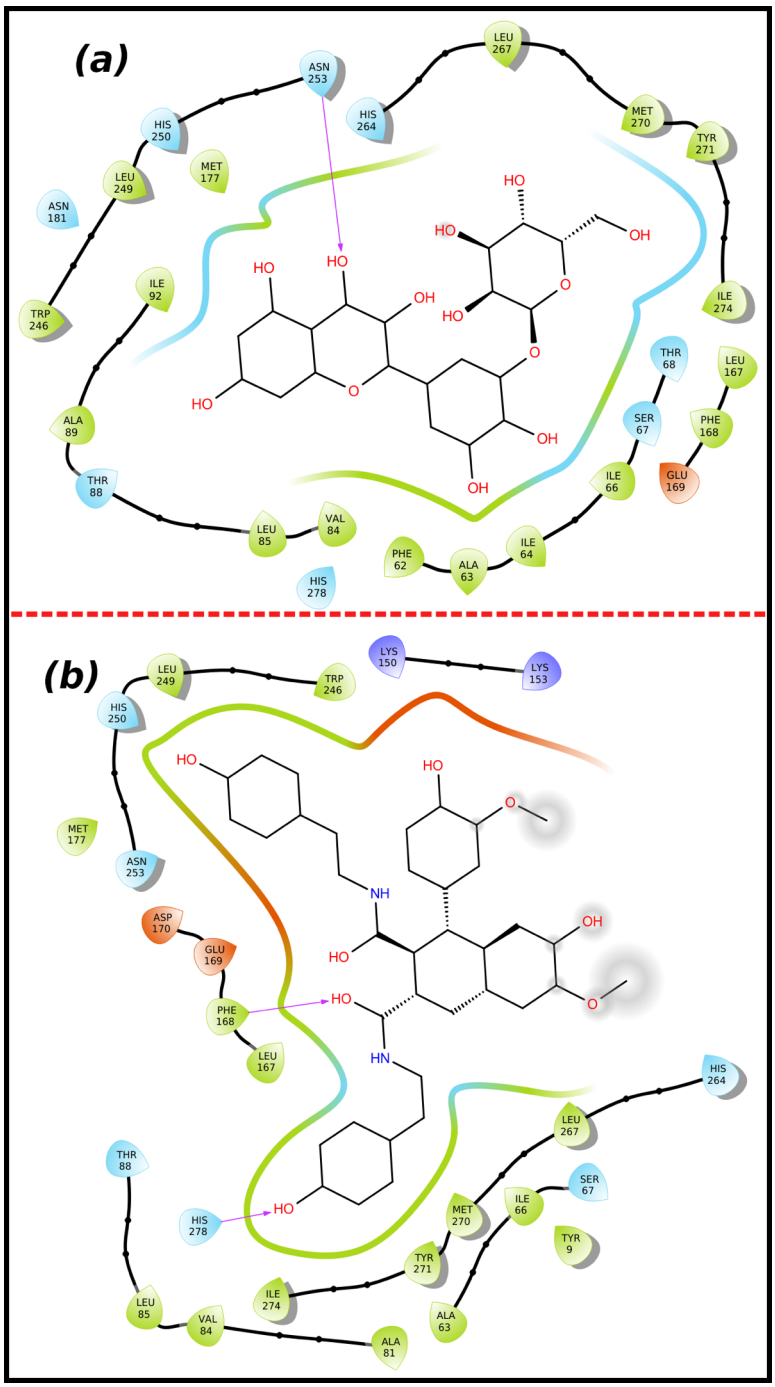

Figure SI-2: Ligad interaction diagram of (a) Cannabiscitrin and (b) Cannabisin D with 2YDO protein.

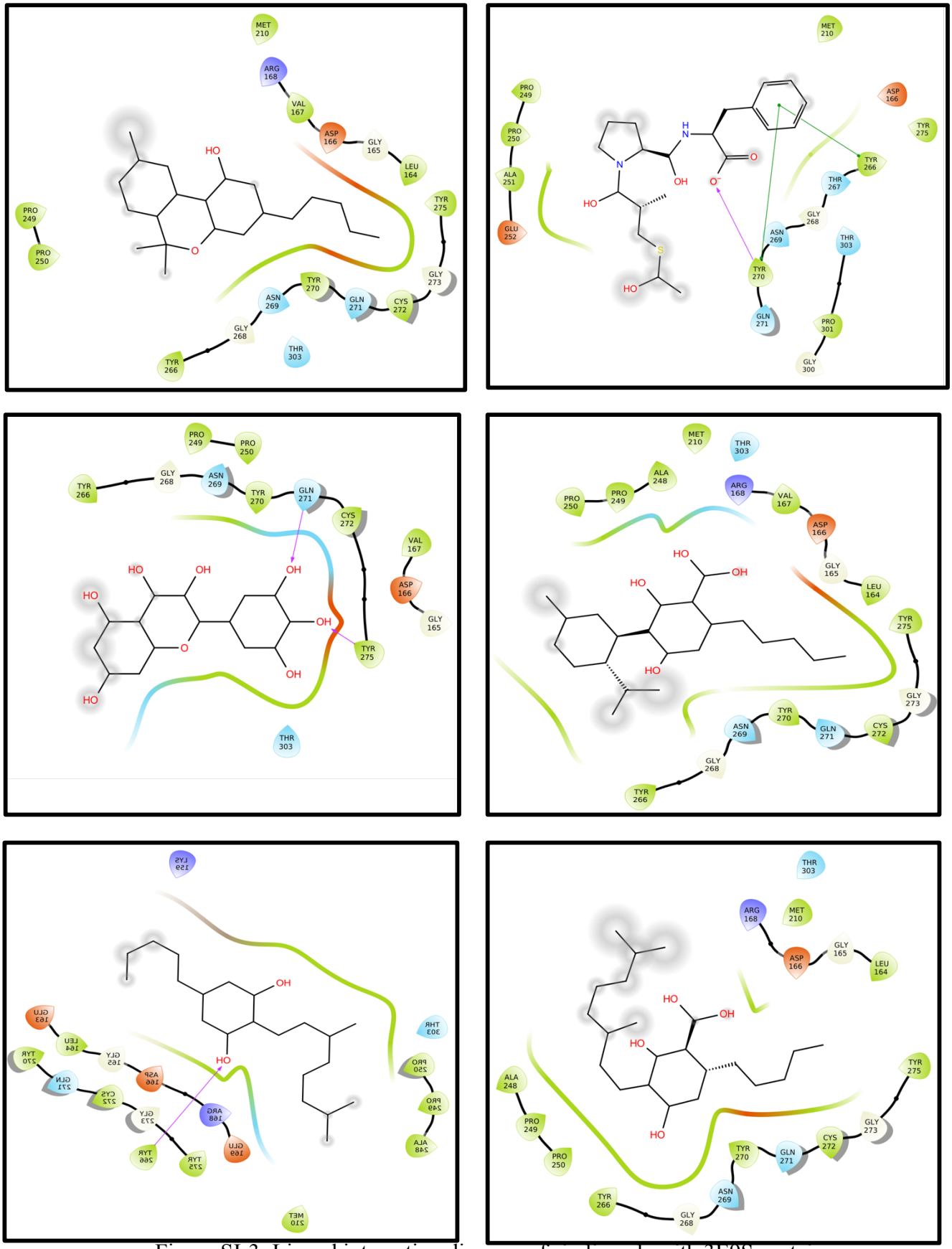

Figure SI-3: Ligand interaction diagram of six ligands with 3E9S protein.

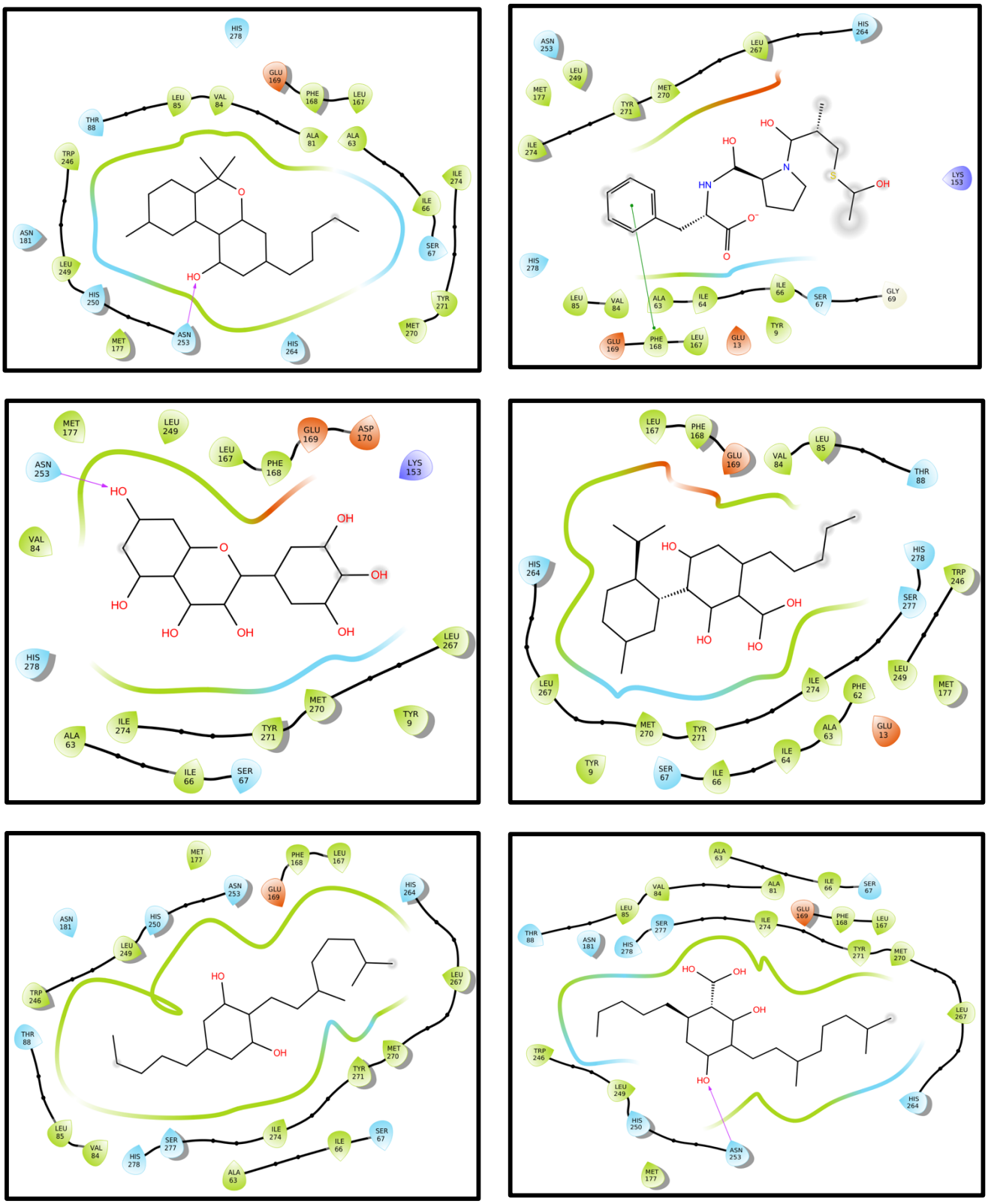

Figure SI-4: Ligand interaction diagram of six ligands with 2YDO protein.

Table SI-1: Interaction Data of ligands with 3E9S protein.

S. No.	Protein_ligand	Hydrophobic Interactions	Hydrogen Bonds	π -π Stacking
1	3E9S_**Cannabinol**	164LEU 166ASP 249PRO 249PRO 270TYR 275TYR		266TYR 270TYR
2	3E9S_**Alacepril**	267THR 301PRO		
3	3E9S_**Myricetin**	250PRO 270TYR	266TYR 268GLY 269ASN 271GLN 275TYR	266TYR
4	3E9S_**Cannabidiol Acid**	164LEU 166ASP 249PRO 266TYR 275TYR	268GLY	270TYR
5	3E9S_**Cannabigerol**	166ASP 249PRO 266TYR 271GLN 303THR	266TYR 270TYR 270TYR 271GLN	270TYR
6	3E9S_**Cannabigerolic Acid**	166ASP 266TYR 270TYR 271GLN	268GLY	270TYR Salt Bridges 168ARG
7	3E9S_**Cannabiscitrin**	62PRO 68ARG 71ALA 82PHE 83LEU	77THR 83LEU	π-Cation Interactions 68ARG
8	3E9S_**Cannabisin D**	249PRO 250PRO 266TYR 270TYR 271GLN 275TYR	164LEU 169GLU 270TYR	π-Cation Interactions 168ARG

Table SI-2: Interaction Data of ligands with 2YDO protein.

S. No.	Protein_ligand	Hydrophobic Interactions	Hydrogen Bonds	π -π Stacking
1	2YDO_**Cannabinol**	63ALA 167LEU 168PHE 246TRP 249LEU 274ILE	253ASN	168PHE
2	2YDO_**Alacepril**	167LEU	153LYS	
3	2YDO_**Myricetin**	168PHE 249LEU 274ILE	63ALA 253ASN 271TYR	168PHE
4	2YDO_**Cannabidiol Acid**	84VAL 168PHE 169GLU 267LEU 270MET 271TYR 274ILE	9TYR 66ILE	
5	2YDO_**Cannabigerol**	84VAL 85LEU 88THR 167LEU 168PH 169GLU 246TRP 249LEU 267LEU 270MET 274ILE	253ASN	168PHE
6	2YDO_**Cannabigerolic Acid**	85LEU 167LEU 168PHE 169GLU 246TRP 267LEU 274ILE	253ASN	168PHE Salt Bridges 278HIS

7	2YDO_**Cannabiscitrin**	168PHE 246TRP 249LEU 274ILE	66ILE 169GLU 253ASN	168PHE
8	2YDO_**Cannabisin D**	66ILE 84VAL 167LEU 168PHE 169GLU 249LEU 267LEU 274ILE	150LYS 153LYS 168PHE 169GLU 253ASN 278HIS	168PHE

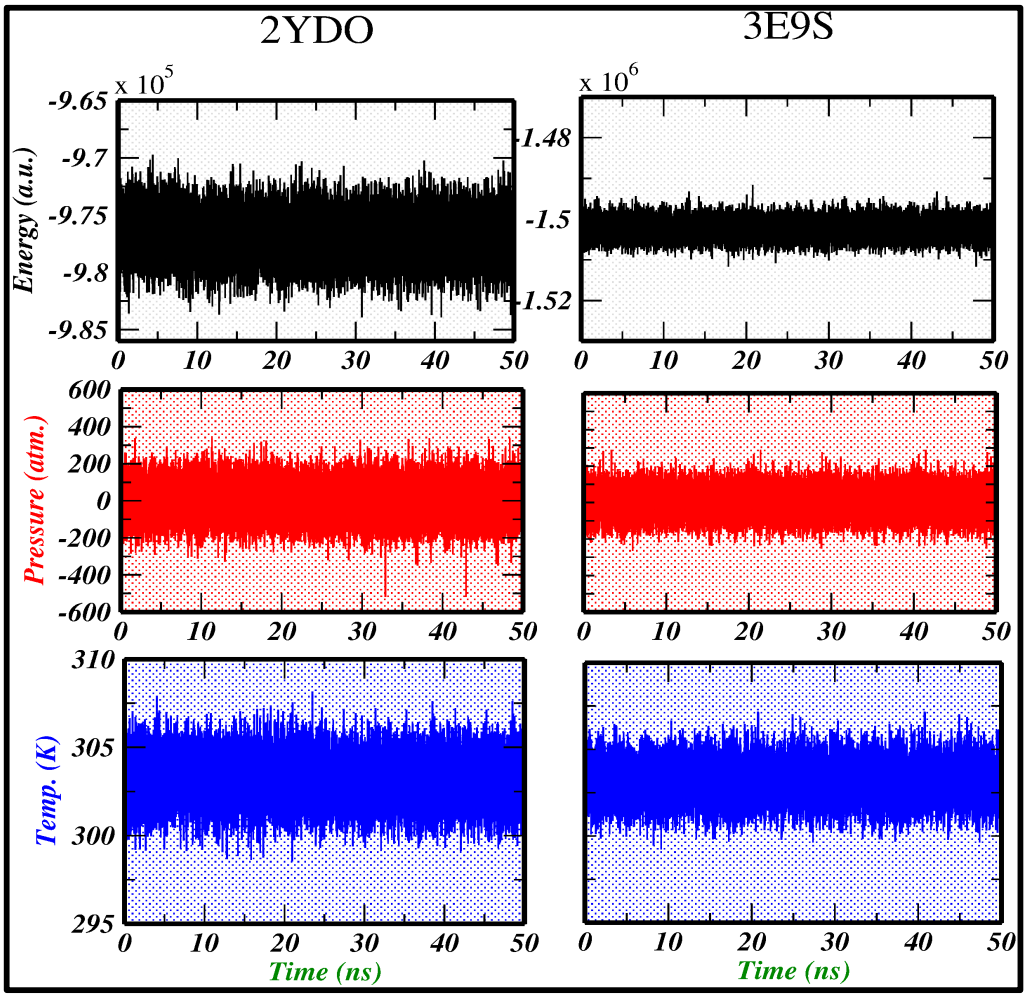

Figure SI-5: Variation of Energy, Pressure and Temperature along the simulation trajectory for both 2YDO and 3E9S systems, respectively.